13th World Conference on Earthquake Engineering
Vancouver, B.C., Canada
August 1-6, 2004
Paper No. 2173

PSEUDO-DYNAMIC TEST OF A FULL-SCALE CFT/BRB FRAME: PART 3 - ANALYSIS AND PERFORMANCE EVALUATION

Min-Lang LIN [1], Yuan-Tao WENG[2], Keh-Chyuan TSAI[3], Po-Chien HSIAO[4], Chui-Hsin CHEN [5], and Jiun-Wei LAI [6]

SUMMARY

This is the third of a three-part paper describing a full-scale 3-story 3-bay CFT buckling restrained braced frame (CFT/BRB) specimen that was constructed and tested in the structural laboratory of National Center for Research on Earthquake Engineering (NCREE) in Taiwan using pseudo dynamic test procedures and internet testing techniques in October of 2003. The test frame were loaded to simulate the responses under ground motions corresponding to earthquake hazards for a high-seismicity site with 50%, 10%, and 2% chance of exceedance in 50 years. The frame specimen was designed using displacement-based seismic design (DSD) procedures considering a target inter-story drift limit of 0.025 radian. This paper summarizes the analytical studies of the test frame and evaluates the test responses. Inelastic static and dynamic time history analyses were conducted using OpenSees and PISA3D, developed at Pacific Earthquake Engineering Research Center (PEER) and National Taiwan University, respectively. CFT/BRBF performed extremely well after the application of six earthquake load effects. Very minor changes on stiffness and damping are observed as evidenced from the free vibration tests conducted after each earthquake pseudo dynamic test. The peak story drift reached 0.023 radian at the first story after applying the 2/50 design earthquake on the specimen. Tests confirmed that the DSD procedure adopted in the design of the specimen is effective in limiting the ultimate story drift under the effects of the design earthquake. Tests also confirmed that the response of the CFT/BRB frame can be satisfactorily predicted by using either OpenSees or PISA3D.

---

[1] Associate Research Fellow, National Center for Research on Earthquake Engineering, 200, Sec.3, Hsinhai Rd., Taipei 10658, Taiwan, ROC, Email: mllin@ncree.gov.tw,
[2] Postdoctoral Researcher, National Center for Research on Earthquake Engineering, 200, Sec.3, Hsinhai Rd., Taipei 10658, Taiwan, ROC, Email: d88521003@ms88.ntu.edu.tw
[3] Director, National Center for Research on Earthquake Engineering, 200, Sec.3, Hsinhai Rd., Taipei 10658, Taiwan, ROC, Email: kctsai@ncree.gov.tw,
[4] Graduate student, National Taiwan University, Email: r91521221@ntu.edu.tw
[5] Assistant Research Fellow, National Center for Research on Earthquake Engineering, 200, Sec.3, Hsinhai Rd., Taipei 10658, Taiwan, ROC, Email: chchen@ncree.gov.tw
[6] Research Assistant, National Center for Research on Earthquake Engineering, 200, Sec.3, Hsinhai Rd., Taipei 10658, Taiwan, ROC, Email: jwlai@ncree.gov.tw

INTRODUCTION

Through international collaboration between researchers in Taiwan, Japan, and the United States, a full-scale 3-story 3-bay RC column and steel beam RCS composite moment frame was tested in October of 2002 in the structural laboratory of National Center for Research on Earthquake Engineering (NCREE) in October 2002 [1]. In the year 2003, a full-scale 3-story 3-bay CFT column with the buckling restrained braced composite frame (CFT/BRBF) specimen has been tested in October in a similar manner. The 3-story prototype structure is designed for a highly seismic location either in Taiwan or United States. The typical bay width is 7m and typical story height is 4m. The total height of the frame, including the footing, is about 13m. The 2.15 meters wide concrete slab is adopted to develop the composite action of the beams. Measuring 12 meters tall and 21 meters long, the specimen is among the largest frame tests of its type ever conducted. The frame has been tested using the pseudo-dynamic test procedures applying input ground motions obtained from the 1999 Chi-Chi and 1989 Loma Prieta earthquakes, scaled to represent 50%, 10%, and 2% in 50 years seismic hazard levels. Following the pseudo-dynamic tests, since none of the brace was fractured, quasi static loads have been applied to cyclically push the frame to large inter-story drifts up to the failure of the braces, which will provides valuable data to validate possible failure mechanism and analytical models for large deformation response. Being the largest and most realistic composite CFT/BRB frame ever tested in a laboratory, the test provides a unique data set to verify both computer simulation models and seismic performance of CFT/BRB frames. This experiment also provides great opportunities to explore international collaboration and data archiving envisioned for the Networked Earthquake Engineering Simulation (NEES) initiatives or the Internet-based Simulations for Earthquake Engineering (ISEE) [2] launched recently in USA and Taiwan, respectively. This paper focuses on the displacement-based seismic design procedures adopted in the design of CFT/BRB frame specimen. During the planning stage, extensive nonlinear dynamic analyses were also carried out in order to ensure the possible seismic demands would not exceed the force and displacement limits of the test facility. This paper describes the experimental and analytical results and evaluates the seismic performance of the frame specimen observed from the measured test responses. Inelastic static and dynamic time history analyses have been conducted using PISA3D[3] and OpenSees (Open System for Earthquake Engineering Simulation, http://opensees.berkeley.edu), developed at National Taiwan University and Pacific Earthquake Engineering Research Center (PEER), respectively.

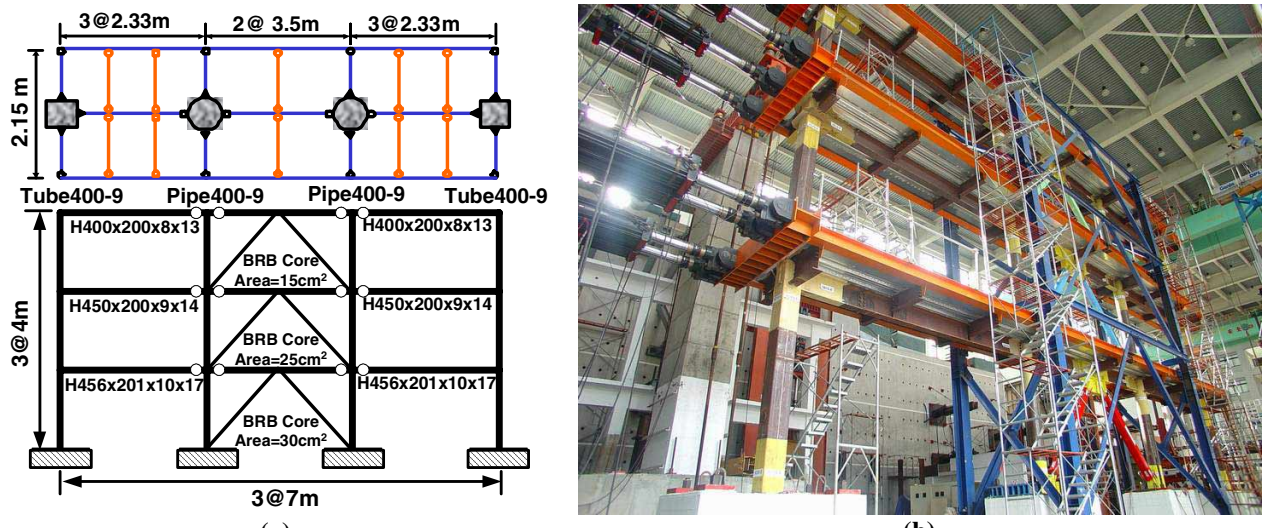

Fig. 1 (a) Plan and elevation of the full-scale CFT/BRB composite frame
(b) Photo of the CFT/BRB test frame

Table 1 Selection of member sizes and grades

Member	Beam Sizes and Core Cross Sectional Area of Braces (A572 GR50)		
Location	1FL	2FL	3FL
Beam (mm)	H456×201×10×17	H450×200×9×14	H400×200×8×13
Brace (cm^2)	30	25	15
Dimension of Columns (A572 GR50) unit : mm		CFTs: C1: Tube: 350×9, C2: Pipe: 400×400×9	

Table 2 Material test results

		Positions of Sampling		f_y (MPa)	f_u (MPa)
Steel (A572 Gr. 50)	3FL	Beam	Flange	372	468
			Web	426	493
		BRB3	core steel material	373	483
	2FL	Beam	Flange	414	503
			Web	482	538
		BRB2	core steel material	397	545
	1FL	Beam	Flange	370	486
			Web	354	485
		BRB1	core steel material	421	534
Tube 400-9		Steel		374	488
		Concrete		f_c'=35 MPa	
Pipe 400-9		Steel		543	584
		Concrete		f_c'=35 MPa	

A FULL SCALE CFT/BRB COMPOSITE FRAME

The 3-story CFT/BRB frame shown in Fig. 1 is employed in this experimental research. The prototype three-story building consists of 6-bay by 4-bay in plane. In the two identical prototype CFT/BRB frames, only the two exterior beam-to-column joints (Fig. 1) in each floor are moment connections, all other beam-to-column connections are assumed not to transfer any bending moment. The BRBs are installed in the center bay. Square CFT columns are chosen for the two exterior columns while the center two columns are circular CFTs. Story seismic mass is 31.83 ton for the 1st and 2nd floors, 25.03 ton for the 3rd floor for each CFT/BRB frame (half of the building). All steel is A572 GR50 with yield strength of 350 MPa and the infill concrete in the CFT columns are 35 MPa. The displacement-based seismic design (DSD) procedures proposed by others [4,5] assuming that the CFT/BRB frame specimen vibrates essentially in a single mode were adopted. The DSD details of the specimen can be found in the the references [6,7] and in the companion paper [8]. The final selections of structural members are given in Table 1. It considers the actual material coupon strength as given in Table 2.The material is A572 Gr.50 for all the steel beams and columns, while the compression strength fc' of the concrete filled in CFT columns is 35MPa. The supporting beams above the BRBs satisfy the capacity design principal considering the strained hardened BRBs and an unbalanced vertical load resulted from the difference of the peak BRB compressive and tensile strengths. The fundamental vibration period is about 0.68 second. Three different types of moment connections, namely through beam, external diaphragm and bolted end plate types, varying from the first floor to the third floor were fabricated for the exterior beam-to-column connections. Three types of BRBs, including the single-core, double-cored and the all-metal BRBs, were adopted in the three different floors. In particular, two single-cored unbonded braces (UBs), each consisting of a steel flat plate in the core, were donated by Nippon Steel Company and installed in the second floor. Each UB end to gusset

connection uses 8 splice plates and 16-24mmϕ F10T bolts. The two BRBs installed in the third story are double-cored constructed using cement motar infilled in two rectangular tubes [9] while the BRBs in the first story are also double-cored but fabricated with all-metal detachable features [10]. Each end of the double-cored BRB is connected to a gusset plate using 6- and 10-24mmϕ F10T bolts at the third and first floor, respectively. No stiffener was installed at the free edges of any gusset before the testing.

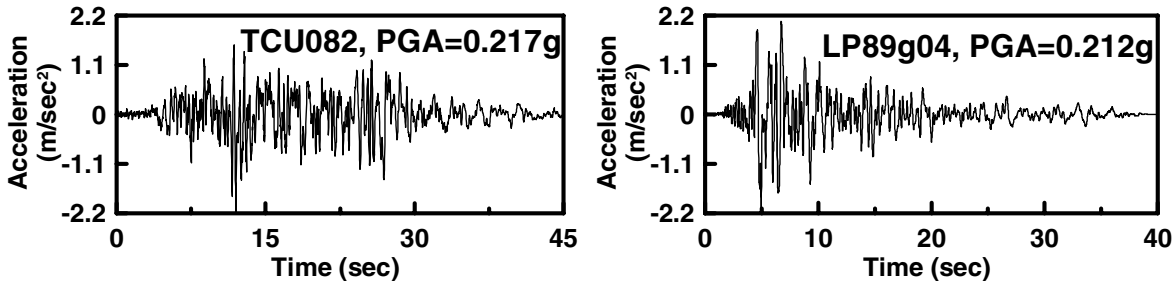

Fig. 2 Original ground accelerations used in test (before scaling)

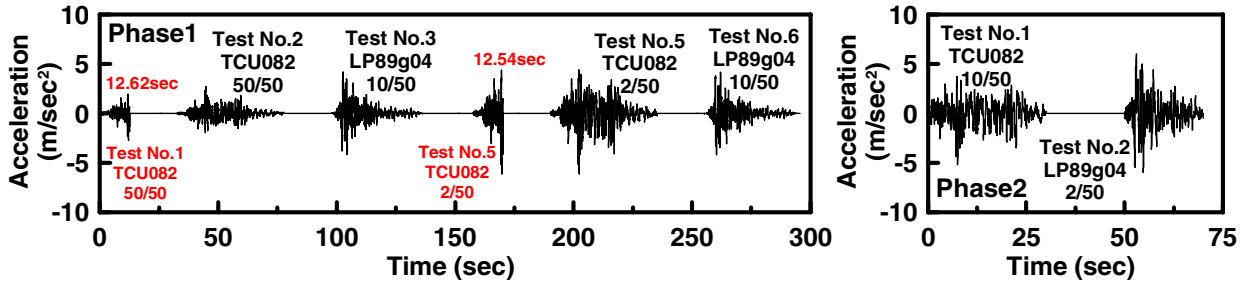

Fig. 3 Ground acceleration time history in PDTs

EXPERIMENTAL PROGRAM

The experimental program utilizes PDT procedures to simulate the earthquake load effects imposed on the test structure. Based on the results of the pre-test analyses, conducted using PISA3D and OpenSees, two earthquake records were chosen among strong motion records collected during recent earthquakes. As shown in Fig.2, the two earthquake records are TCU082-EW (from the 1999 ChiChi earthquake) and LP89g04-NS (from the 1989 Loma Prieta earthquake), both of which are considered to represent general motions without near-field directivity effects. The original test plan was to scale these two records in acceleration amplitude to represent four separate pseudo-dynamic loading events, which were sequenced as follow: (1) TCU082 scaled to represent a 50/50 hazard intensity, i.e., with a 50% chance of exceeding in 50 years, (2) LP89g04 scaled to a 10/50 hazard intensity, which represents the design basis earthquake, (3) TCU082 scaled to a 2/50 hazard, and (4 LP89g04 scaled to a 10/50 hazard – identical to loading (2). The records scaling is based on matching their spectral acceleration at the first mode frame period to the specified earthquake hazard levels.

Fig.3 shows the actual applications of the ground motions in the PDTs for the CFT/BRB frame specimen. As noted above, four earthquake ground accelerations scaled to three different PGAs were planned for the PDT of the CFT/BRB frame specimen. However, some unexpected events encountered during the testing. In the Test No. 1, due to the buckling of the gusset plate occurred at the brace to beam connection in the first story, the test stopped at the time step of 12.3 second. Then stiffeners were added at the free edges of all the gusset plates underneath the floor beams. Then test resumed using the same ground accelerations as Test No.1 in reversed direction. In test No.4, the PDT test was stopped at the time step of 12.54 second

due to the crack on the top of concrete foundation near the gusset plate for the south BRB-to-column joint were observed. After one pair of angles was installed bracing the stiffener to the two anchoring steel blocks, the test resumed again by applying the same earthquake acceleration as that for Test No.4. A total of six PDTs were conducted before the final cyclic loading test. After the pseudo dynamic tests, all the BRBs were not damaged. Therefore, cyclic increasing story drifts were imposed until the failure of the BRBs. Since the scheduled PDT and cyclic tests were completed with failures only in bracing components including the BRBs, UBs and the gusset plates, it was decided that Phase-2 tests be conducted after repairing the damaged components. Due to the buckling to the gusset plates observed in the brace-to-column joints in the Phase-1 tests, additional stiffeners were added at the free edges of the gusset at the two third floor brace-to-column joints after the buckled gussets were heat straightened. In addition, the laterally buckled gusset plate under the 3rd floor beam was removed before installing a new one. Six new BRBs, two all metal double cored construction for the 1st story, four concrete filled double cored for the 2nd and 3rd stories, have been installed. Phase-2 tests not only allowed to make the best use of the 3-story, 3-bay frame but also aimed to investigate the performance of the stiffened gussets plates and the new BRBs. The ground motion accelerations applied in Phase 2 PDTs are also shown in Fig. 3. Details of the observation and discussion for the PDTs are summarized in the companion paper [11].

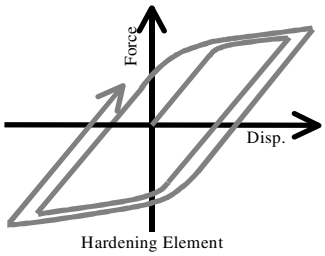

Fig. 4 Two-surface plasticity hardening truss element

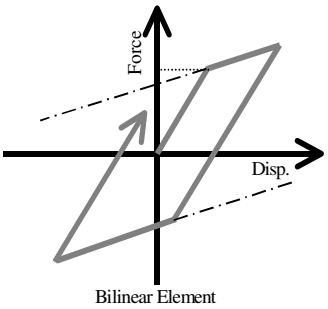

Fig. 5 Bilinear element model

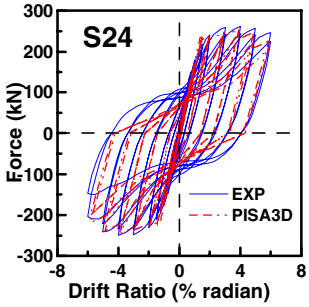

Fig. 6 Drift ratio and force hysteresis of CFT column

ANALYTICAL MODELS

Extensive analytical studies were performed on the frame specimen prior to the actual test. Inelastic static and dynamic time history analyses were conducted using OpenSees and PISA3D [3]. OpenSees is an objected-oriented simulation framework developed by researchers in the PEER Center for simulating the seismic response of structural and geotechnical systems. Another inelastic simulation and analytical platform PISA3D is developed by the researchers in the National Taiwan University [3].

PISA3D model

All BRBs were modeled using the two-surface plastic (isotropic and kinematic) strain hardening truss element (Fig. 4). All the beam members were modeled using the bi-linear beam-column elements (Fig. 5). Consider the strength degrading behavior of the concrete, All the columns members was modeled using he three-parameter degrading beam-column elements [3]. It is evident that the hysteretic behavior of CFT column members simulated by PISA3D shown at Fig.6 is satisfactory and well agree with the experimental results obtained in the DSCFT column specimen S24 cyclic load test [12]. A leaning column is introduced in the frame model in order to simulate the 2nd order effects developed in the gravity columns.

OpenSees Model

All the CFT columns and steel beams of the frame are modeled by the flexibility-based nonlinear beam-column fiber elements with discretized fiber section model as illustrated in Fig. 7. The uniaxial bilinear steel material model (Steel01 material) is the basic model that incorporates isotropic strain hardening adopted in the analyses. The uniaxial Kent-Scott-Park concrete material model (Concrete01 material) is adopted and no tensile concrete strength is considered. All BRBs were modeled using the truss element. And the Menegotto-Pinto steel material (Steel02 material) with isotropic and kinematic strain hardening was used for the truss element. A leaning column arrangement has also been adopted in OpenSees model. The frame model presented in this paper utilizes the measured material properties of steel beams, CFT tubes, and infilled concrete for the CFT columns as shown in Table 2.

Elements Verification

Cyclic analyses on basic elements are exercised to verify the differences of the elements adopted in PISA3D and OpenSees. Cyclic axial displacement history given in Fig. 8 was applied to two different truss elements in order to validate the analytical BRB models. It is evident that the hysteretic behavior of BRB member simulated either by PISA3D or OpenSees shown at Fig.9 is satisfactory and well agree with the experimental results obtained in a NTU test using A572 Gr.50 BRB [10]. Similarly, in order to compare the three-parameter degrading beam-column element implemented in the PISA3D program and the fiber CFT beam-column models in the OpenSees program, the results of simulating the strength degrading and hysteretic behaviors of the DSCFT column specimen S24 shown at Fig. 9. In addition, since most of the story shear is resisted by the braces, preliminary analyses have confirmed that the effects of the CFT column hysteretic behavior are rather insignificant.

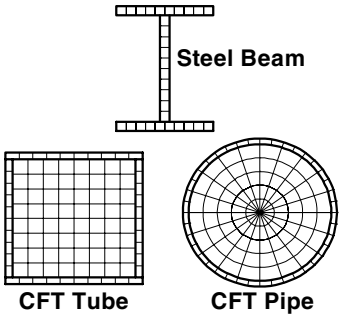

Fig. 7 Fiber sections in OpenSees

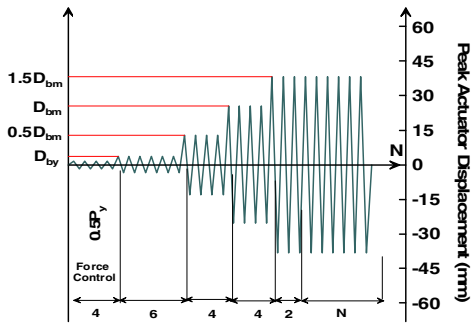

Fig. 8 Cyclic axial displacement history for two-surface plasticity brace element (core length=1700mm)

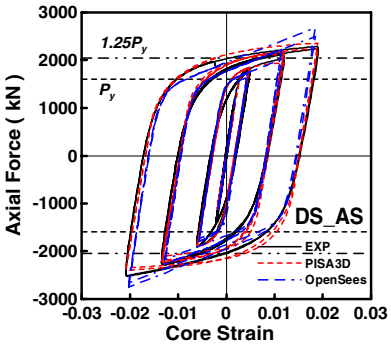

Fig. 9 BRB element models

ANALYTICAL VERSUS EXPERIMENTAL RESULTS AND DISCUSSIONS

Fig. 10 and Fig. 11 give the analytical and experimental roof displacement time history and peak story displacement distributions of CFT/BRB frame specimen imposed in the Phase 1 and Phase 2 PDTs. It is evident that the lateral displacements of CFT/BRB frame predicted either by OpenSees or Pisa3D are satisfactory. Table 3 shows the maximum and minimum lateral displacements of the predicted and measured response for Phases1 and 2 PDTs. The peak roof displacement is about 24.2cm which occurred in Test No.2 (2% in 50 years seismic hazard level) of Phase 2. The differences between the analytical and experimental responses are also shown in Table 3.

Table 3 Roof displacement comparisons and differences

Events		Lateral Displacement (cm)						Error (%)			
		TEST		OpenSees		PISA3D		OpenSees		PISA3D	
		max	min	max	min	max	Min	max	min	max	min
Phase1	Test No.2	4.9	-7.0	5.9	-7.4	5.9	-7.7	17	5	17	9
Phase1	Test No.3	11.7	-17	11.3	-15.5	7.5	-17.4	4	10	56	2
Phase1	Test No.5	20.8	-12.9	21.5	-13.8	21.8	-10.8	3	7	5	19
Phase1	Test No.6	18	-13.2	15.3	-10	16.8	-7.1	18	32	7	86
Phase2	Test No.1	20.2	-11.9	18.7	-10.4	18.6	-6.5	8	14	9	83
Phase2	Test No.2	16.7	-24.2	17.9	-23.1	17.4	-23.3	7	5	4	4

Table 4 Base shear comparison

Events		Story Shear (10^3kN)						Error (%)			
		TEST		OpenSees		PISA3D		OpenSees		PISA3D	
		max	min	max	min	max	min	max	min	max	min
Phase1	Test No.3 10/50	2.7	-3.1	2.4	-2.6	-2.8	2.4	13	19	13	11
Phase1	Test No.5 2/50	3.6	-3.3	3.3	-3.4	3.4	-3	9	3	6	10
Phase2	Test No.2 2/50	2.9	-3.0	3.1	-3.1	2.9	-2.9	6	3	1	5

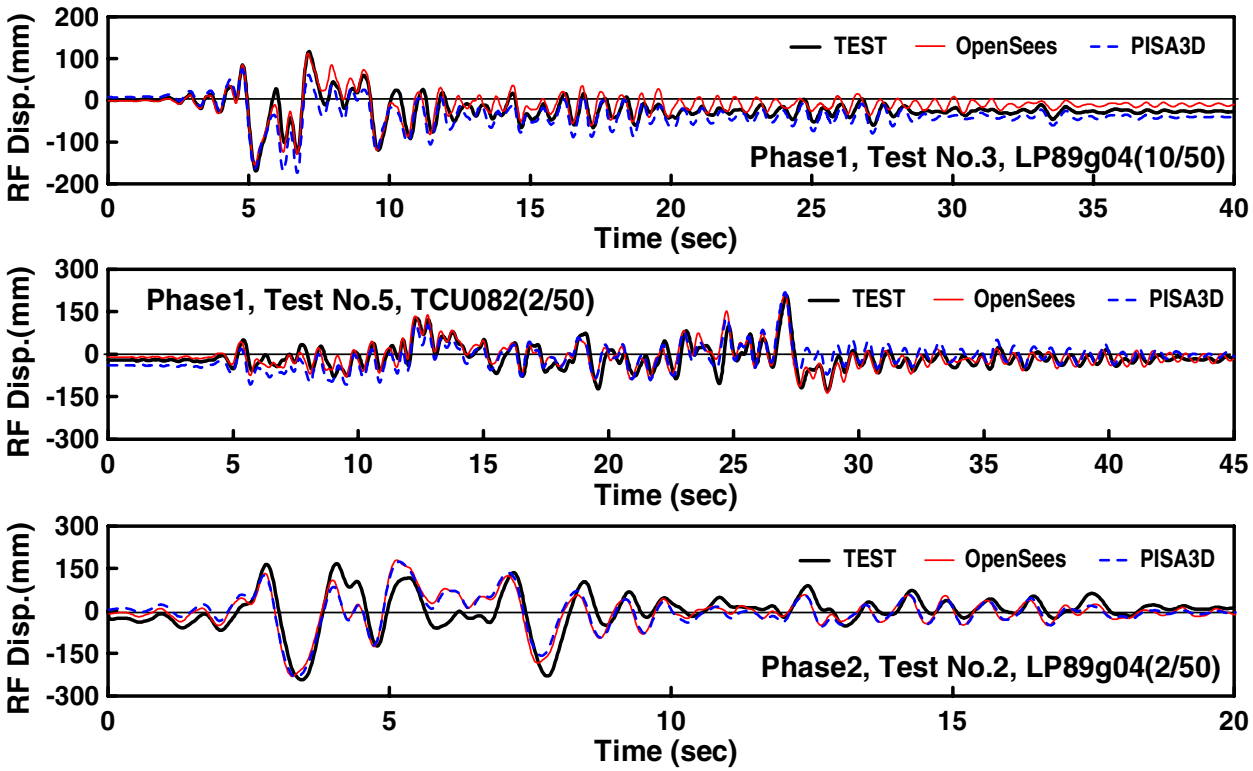

Fig. 10 Roof displacement history in Tests

Fig. 12 and Fig. 13 show that the predicted values agree well with the experimental story shear time history response and the peak story shears. As shown in Table 4, it's found that the maximum story shear differences between the prediction and the test result are 19% and 13% for OpenSees and PISA3D, respectively. The story drift versus story shear hysteresis responses are shown in Fig. 14. In the Test No.3 (the 10/50 event), the maximum inter-story drift occurred at the first floor is 1.9% radian, very close to the design limit of 2% radian. And during the 2/50 event (Test No.5), the maximum inter-story drift occurred at first floor is 2.3% radian, also very close to the design limit of 2.5% radian. The peak frame deformational responses have well met the drift limit prescribed in the target performance level defined in the displacement-based design procedures.

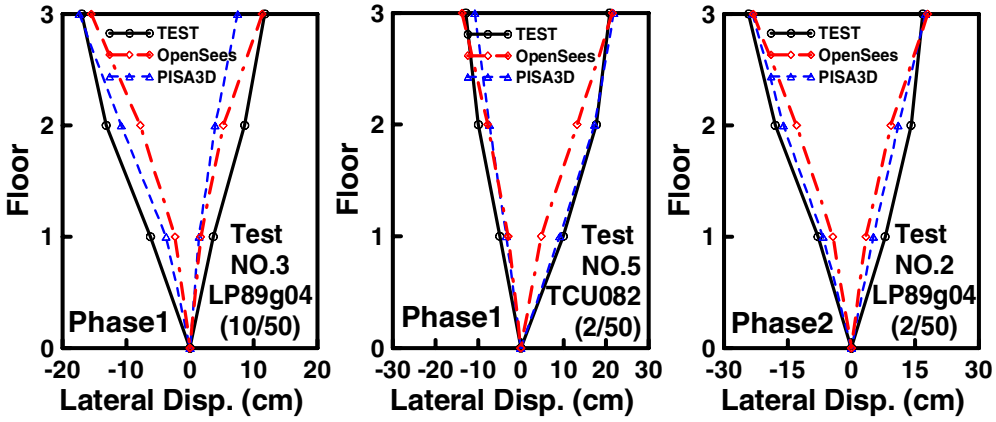

Fig. 11 Peak story displacement distribution

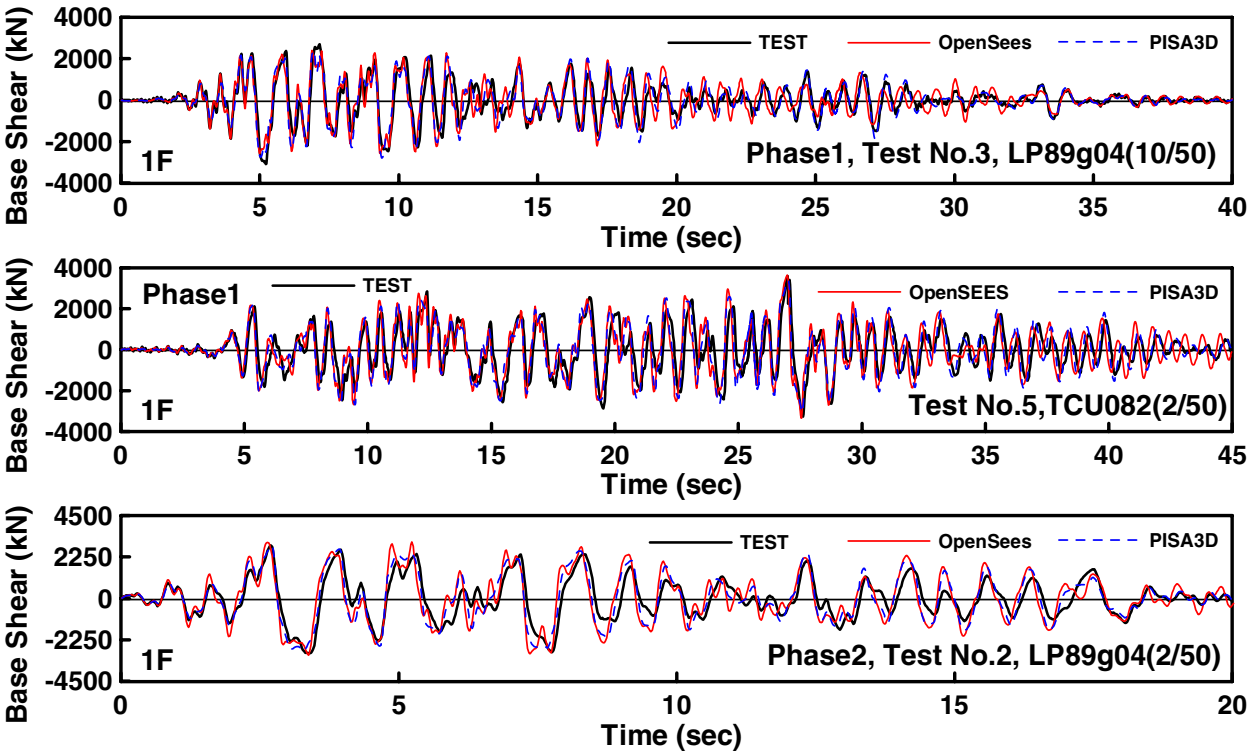

Fig. 12 Base shear history in Tests

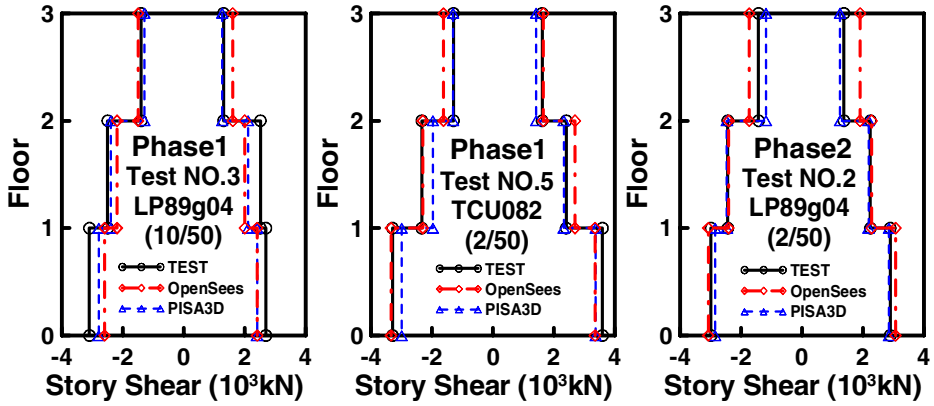

Fig. 13 Peak story shear distribution of CFT/BRB frame specimen

Table 5 South BRB axial force Comparison

Phase1		South BRB Axial Force (10^3kN)						Error (%)			
		TEST		OpenSees		PISA3D		OpenSees		PISA3D	
		max	min	max	min	max	Min	max	min	max	min
Test No.3 10/50	RF	0.63	-0.73	0.78	-0.86	0.77	-0.82	19	15	18	11
	2F	1.18	1.17	1.23	-1.35	1.32	-1.46	4	13	11	20
	1F	1.36	-1.38	1.32	-1.42	1.47	-1.65	3	3	7	16
Test No.5 2/50	RF	0.63	-0.82	0.89	-0.89	0.76	-0.84	29	8	17	2
	2F	1.00	-1.4	1.48	-1.45	1.4	-1.52	32	3	29	8
	1F	1.38	-1.72	1.5	-1.54	1.64	-1.81	8	12	16	5

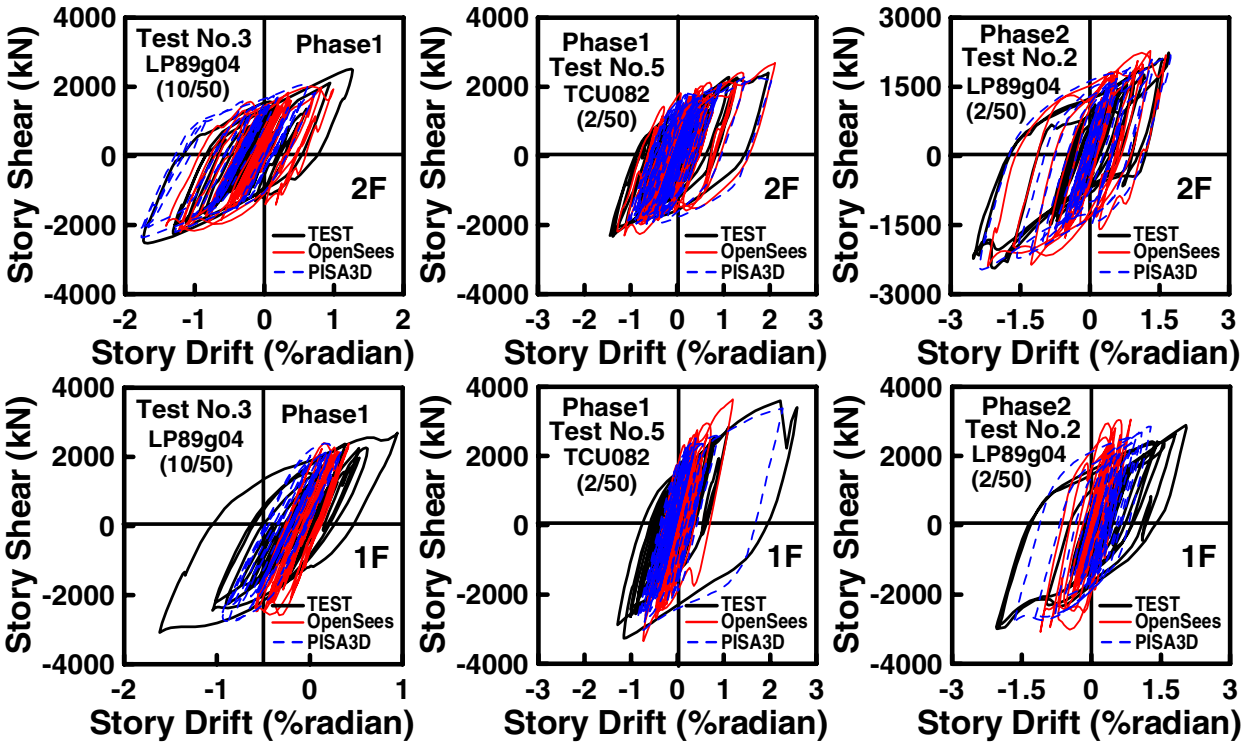

Fig. 14 Story drift and story shear hysteresis

Table 6 North BRB axial force Comparison

Phase1		North BRB Axial Force (10^3kN)						Error (%)			
		TEST		OpenSees		PISA3D		OpenSees		PISA3D	
		max	min	max	min	max	Min	max	min	max	min
Test No.3 10/50	RF	0.71	-0.72	0.79	-0.86	0.75	-0.83	10	16	5	13
	2F	1.26	-1.29	1.27	-1.32	1.37	-1.42	1	2	8	9
	1F	1.48	-1.5	1.34	-1.41	1.49	-1.64	10	6	1	9
Test No.5 2/50	RF	0.64	-0.83	0.82	-0.96	0.76	-0.87	22	14	16	5
	2F	1.24	-1.34	1.36	-1.56	1.37	-1.55	9	14	9	14
	1F	1.51	-1.93	1.45	-1.59	1.71	-1.79	4	21	12	8

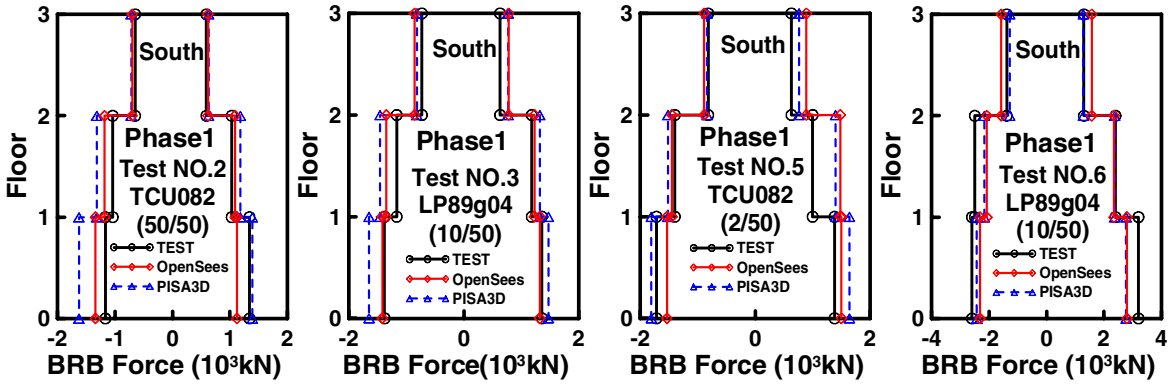

Fig. 15 Peak South brace axial force distribution

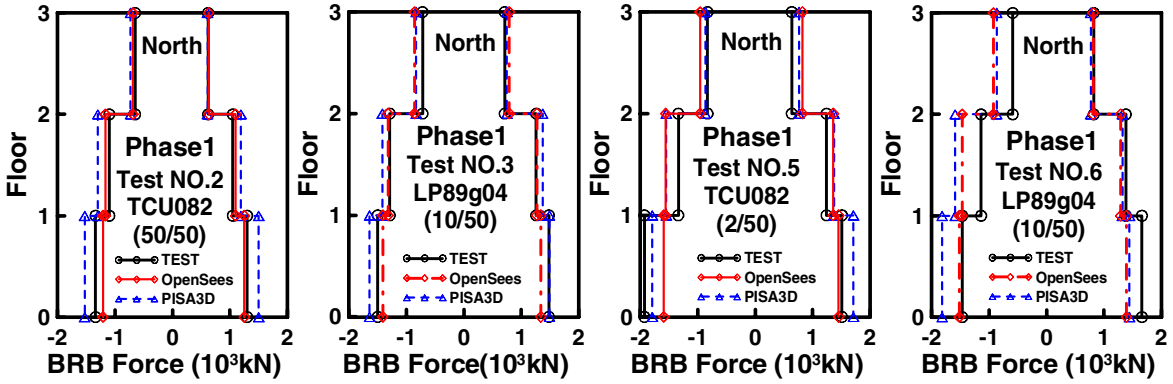

Fig. 16 Peak North brace axial force distribution

In order to obtain the strain gauge reading and axial force relationship of the brace members, there are eight uniaxial strain gauges arranged in the both ends of each brace. Before the installation of the braces, the elastic member test was conducted for each UB and BRB. The linear relationship between the axial forces and starin readings was computed from the elastic member tests, therefore the corresponding axial force reading can be found during the PDTs immediately. Tables 5 and 6 show the peak predicted and experimental axial forces of the BRBs and UBs. Figs. 15 and 16 show the peak brace axial force distributions for BRBs and UBs. It's found that either the BRBs or the UBs sustained the ultimate axial forces equally in tension and compression. The maximum differences between the peak predicted and experimental axial forces are 32% and 29% for OpenSees and PISA3D, respectively.

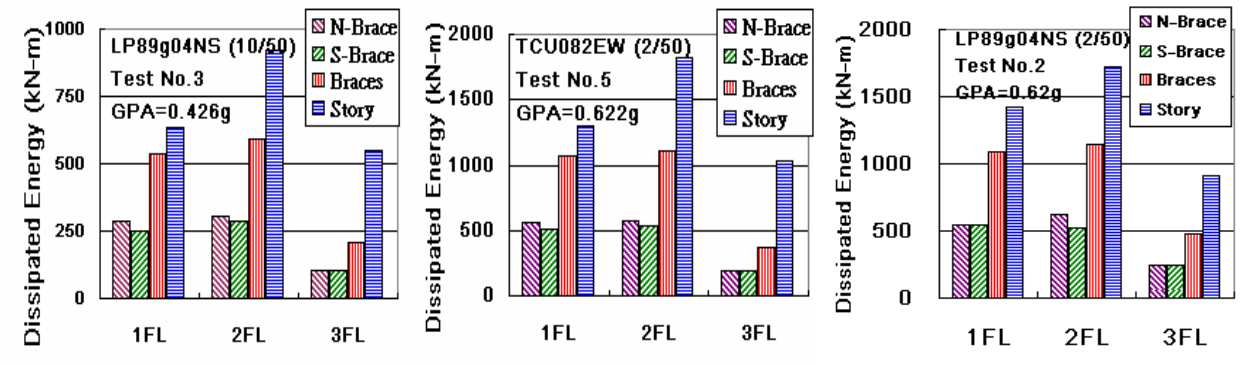

Fig. 17 Comparison of Dissipated energy in Tests

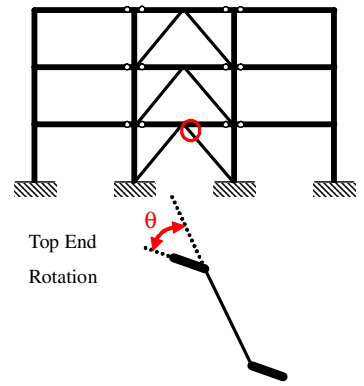

Fig. 18 Definition of top brace end rotation

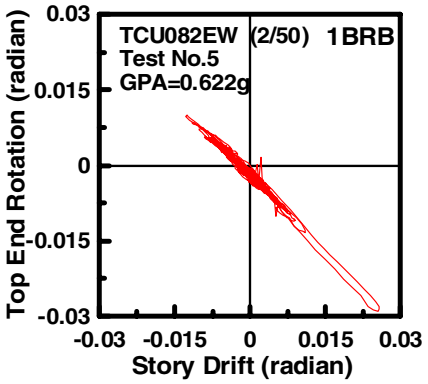

Fig. 19 Top end rotation and Story drift hysteresis in Phase1, Test No. 5

In the Test No. 2 in Phase 1, braces started to experience plastic deformation at the first and the second floors. As shown in Table 7, by computing the linear responses between the axial force and core displacement of braces before yielding, it is confirmed that the initial stiffness of the BRBs of the specimen is rather close to the design value. This suggests that the unbonding mechanism of the BRBs is effective in these BRBs. After the application of six earthquake effects in Phase 1 tests, it is found that the UBs and BRBs performed rather satisfactorily without evident failure. Further more, the BRBs dissipated most of hysterestic energy absorbed by the structure in different levels of earthquake intensities (Fig. 17). In each case, the energy dissipated by the north BRB is almost the same as that by the south BRBs in each floor suggesting the accurate transformation of the strain gauge readings into the brace axial forces. In the meantime, the ultimate story drift of the BRB composite frame was controlled rather effectively under the effects of the design earthquakes.

Table 7 Effective stiffness of BRBs or UBs

	Experiment		Analysis		error (%)	
	N (kN/mm)	S (kN/mm)	N (kN/mm)	S (kN/mm)	N	S
3BRB	91.49	87.99	87.35	87.35	4.7	0.7
2UBB	183	181.36	191.10	191.10	4.2	5.1
1BRB	192.96	184.32	185.90	185.90	3.8	0.8

The end rotations θ of the first floor BRBs as defined in Fig. 18 are compared against the story drifts in Test No.5 in Fig. 19. It is evident that the rotational demands imposed on the brace end are significant and

increase with the story drift. It appears that it should be considered in the BRB component tests and in BRB connection design. Further research on the end rotational demand of BRBs is needed.

The ratios between the cumulative inelastic axial deformation and the tensile yield displacement [13], defined as CPD, taken as the plastic deformations occurring in a brace summed over all cycles throughout the entire response history, in either tension or compression, divided by the tensile yield displacement of the BRB brace member, are listed in Table 7. It reaches 95.1 after undergoing the six earthquake events, at one 2nd floor brace. The cumulative deformations computed from the experimental results show that the BRBs at the 2nd floors are much more vulnerable than those in the 1st and 3rd floor. After the pseudo dynamic tests, all the BRBs were not damaged. Therefore, cyclic increasing story drifts were imposed until the failure of the BRBs. When the BRBs were failed either in fracturing of BRBs or buckling in the gussets [11], the minimum CPD of BRBs is 167 while the maximum is about 212, close to the cumulative ductility capacity observed in the typical BRB component tests [10].

Table 8 CPD of BRB members obtained in pseudo tests

Phase1	Test No. 1 and 2 (50/50)		Test No.3 (10/50)		Test No.4 and 5 (2/50)		After Cyclic Loading		Summary	
	North	South	North	South	North	South	North	South	North	South
RF	4.40	4.40	14.7	14.5	26.2	26.9	122.0	158.6	167.3	204.4
2F	11.8	12.0	28.9	27.4	54.4	50.6	117.4	114.3	212.5	204.3
1F	8.9	7.4	19.3	16.8	38.0	34.7	117.8	119.0	184	177.9

CONCLUSIONS

Based on the test and analytical results, summary and conclusions are made as follows:

- Since most the story shear is resisted by the BRBs, test results confirm that the global dynamic responses of the 3-story 3-bay CFT-BRB frame specimen can be satisfactorily predicted using both the two analytical models presented herein. This is primarily because the nonlinear responses of the BRB can be accurately represented by the elastic strain hardened constitutive models adopted in the two types of truss elements.
- The peak story drift reached 0.025 radian in Phase 1 tests after applying the 2/50 design earthquake on the specimen. It appears that the DSD procedure adopted in the design of the specimen is effective in limiting the ultimate story drift under the effects of the design earthquake.
- All the moment connections survived all the Phase-1 and Phase-2 tests without failure. The BRBs effectively control the story drift and reduce the nonlinear demand imposed on these moment connections.
- CFT/BRBF performed extremely well after the application of six earthquake load effects. Very minor changes on stiffness and damping are observed as evidenced from the free vibration tests conducted after each earthquake pseudo dynamic test.
- Test confirmed that BRBs dissipated most of hysterestic energy absorbed by the structure in different levels of earthquake intensities. Further more, the energy dissipated by the north BRB is almost the same as that by the south BRBs in each floor suggesting the accurate transformation of the strain gauge readings into the brace axial forces.

ACKNOWLEDGEMENTS

The National Science Council of Taiwan provided the financial support for this experimental research program. Nippon Steel Company donated two unbonded braces which have been installed in the 2nd floor of the frame specimen. The laboratory supports provided by the NCREE are very much appreciated. Valuable suggestions provided by many US, Japanese and Taiwanese researchers on this joint effort are gratefully acknowledged. The detailed list of participants is given in the web site (http://cft-brbf.ncree.gov.tw).

REFERENCES

1. Chen, C.H., Lai, W.C. Cordova, P., Deierlein, G. G. and Tsai, K.C., "Pseudo-Dynamic Test of a Full-Scale RCS Frame: Part 1, Design, Construction and Testing." Proceedings, International Workshop on Steel and Concrete Composite Constructions, Taipei, Oct. 2003.
2. Yang, Y.S., Wang, S.J., Wang, K.J., Tsai, K.C. and Hsieh, S.H., "ISEE: Internet-Based Simulations for Earthquake Engineering Part I: The Database Approach." Proceedings, International Workshop on Steel and Concrete Composite Constructions, Taipei, Oct. 2003.
3. Tsai, K.C., and Lin, B.C., "User Manual for the Platform and Visualization of Inelastic Structural Analysis of 2D Systems PISA3D and VISA3D." Center for Earthquake Engineering Research, National Taiwan University, Report No. CEER/R92-07, 2003.
4. Loeding, S., Kowalsky, M.J., and Priestley, M.J.N., "Displacement-based Design Methodology Applied to R.C. Building Frames." Structural Systems Research Report SSRP 98/08, Structures Division, University of California, San Diego, 1998.
5. Medhekar, M. S. and Kennedy, D. J. L., "Displacement-Based Seismic Design of Buildings-Theory." Engineering Structures, Vol.22, No.3, 2000, p.p. 201-209.
6. Tsai K.C., Weng, Y.T., Lin, M.L., Chen, C.H., Lai, J.W. and Hsiao, P.C., "Pseudo Dynamic Tests of a Full Scale CFT-BRB Composite Frame: Displacement Based Seismic Design and Performance Evaluations." Proceedings, International Workshop on Steel and Concrete Composite Constructions, National Center for Research on Earthquake Engineering, Taipei, Oct. 7-8, 2003.
7. Weng, Y.T., "A Study of Multi-mode Seismic Performance-based Evaluation and Displacement-based Design Procedures." Ph.D. Thesis, Supervised by Prof. Keh-Chyuan Tsai, Department of Civil Engineering, National Taiwan University, Taipei, Taiwan, 2003.
8. Tsai, K.C., Weng, Y.T., Lin, S.L., and Goel, subhash, "Pseudo-Dynamic Test of a Full-Scale CFT/BRB Frame: Part 1- Performance Based Specimen Design." Proceedings of 13th World Conference on Earthquake Engineering, Vancouver, B.C., Canada, Paper No. 750, August 1-6, 2004.
9. Tsai, K.C., Hwang, Y.C., Weng, C.S, Shirai, T, and Nakamura, H., "Experimental Tests of Large Scale Buckling Restrained Braces and Frames." Proceedings, Passive Control Symposium 2002, Tokyo Institute of Technology, Tokyo, December 2002.
10. Tsai, K.C. and Lin, S.L, "A Study of All Metal and Detachable Buckling Restrained Braces." Center for Earthquake Engineering Research, National Taiwan University, Report No. CEER/R92-08, 2003.
11. Chen, C.H., Hsiao, P.C., Lai, J.W., Lin, M.L., Weng, Y.T., and Tsai K.C., "Pseudo-Dynamic Test of a Full-Scale CFT/BRB Frame: Part 3- Construction and Testing." Proceedings of 13th World Conference on Earthquake Engineering, Vancouver, B.C., Canada, Paper No. 2175, August 1-6, 2004.
12. Tsai, K.C., Lin, M.L., Lin, Y.S. and Wei, S.S., "Nonlinear Responses of Double-Skin Concrete Filled Steel Tube Bridge Pier-to-Foundation Joints." Journal of Earthquake Engineering and Engineering Seismology. (in preparation)
13. Sabelli, R., Mahin, S. and Chang, C., "Seismic Demands on Steel Braced Frame Buildings with Buckling-Restrained Braces." Engineering Structures, 2000; 25(2): 655-666.